

Analogies between random matrix ensembles and the one-component plasma in two-dimensions

Peter J. Forrester

Department of Mathematics and Statistics, ARC Centre of Excellence for Mathematical and Statistical Frontiers, The University of Melbourne, Victoria 3010, Australia

Abstract

The eigenvalue PDF for some well known classes of non-Hermitian random matrices — the complex Ginibre ensemble for example — can be interpreted as the Boltzmann factor for one-component plasma systems in two-dimensional domains. We address this theme in a systematic fashion, identifying the plasma system for the Ginibre ensemble of non-Hermitian Gaussian random matrices G , the spherical ensemble of the product of an inverse Ginibre matrix and a Ginibre matrix $G_1^{-1}G_2$, and the ensemble formed by truncating unitary matrices, as well as for products of such matrices. We do this when each has either real, complex or real quaternion elements. One consequence of this analogy is that the leading form of the eigenvalue density follows as a corollary. Another is that the eigenvalue correlations must obey sum rules known to characterise the plasma system, and this leads us to exhibit an integral identity satisfied by the two-particle correlation for real quaternion matrices in the neighbourhood of the real axis. Further random matrix ensembles investigated from this viewpoint are self dual non-Hermitian matrices, in which a previous study has related to the one-component plasma system in a disk at inverse temperature $\beta = 4$, and the ensemble formed by the single row and column of quaternion elements from a member of the circular symplectic ensemble.

1 Introduction

In random matrix theory there are a number of distinguished ensembles — the classical cases — for which the eigenvalue probability density function (PDF) can be calculated explicitly. For example, the classical Gaussian orthogonal ensemble consisting of real symmetric matrices $\frac{1}{2}(X + X^T)$, where X is an $N \times N$ standard real Gaussian matrix, has its joint eigenvalue PDF proportional to

$$\prod_{l=1}^N e^{-\frac{1}{2}\lambda_l^2} \prod_{1 \leq j < k \leq N} |\lambda_k - \lambda_j|. \quad (1.1)$$

This explicit expression was known to Wigner (see [63] and references therein).

Wigner [72] (reprinted in [63]) also observed that (1.1), upon being written in the form $e^{-\beta U}$, is identical to the Boltzmann factor for the classical gas in one-dimension with total potential energy

$$U = \frac{1}{2} \sum_{l=1}^N \lambda_l^2 - \sum_{1 \leq j < k \leq N} \log |\lambda_k - \lambda_j|, \quad \lambda_l \in \mathbb{R}, \quad (1.2)$$

interacting at inverse temperature $\beta = 1$. The first term in (1.2) represents an harmonic attraction towards the origin, and the second is a pairwise logarithmic repulsion between the particles in the gas. The pair potential

$$-\log |z - w|, \quad (1.3)$$

with $z, w \in \mathbb{C}$, is well known as the solution of the two-dimensional Poisson equation with free boundary conditions, and thus the pair interaction in (1.2) is that experienced by N two-dimensional unit charges confined to a line. To understand the origin of the one-body term $\frac{1}{2}\lambda^2$ from this perspective, suppose there is a smeared out neutralising background charge density $-\sigma(\lambda)$, supported on the interval $[-L, L]$. The one-body term must be the electrostatic energy created by this background charge, and thus we must have

$$\frac{1}{2}\lambda^2 + C = \int_{-L}^L \sigma(y) \log |\lambda - y| dy, \quad \lambda \in [-L, L], \quad (1.4)$$

for some constant C independent of λ . The solution of this integral equation, with the requirement that $\sigma(y)$ vanishes at $y = \pm L$ is (see e.g. [25, Prop. 1.4.3])

$$\sigma(y) = \frac{L}{\pi} \sqrt{1 - (y/L)^2}. \quad (1.5)$$

Charge neutrality requires $\int_{-L}^L \sigma(y) dy = N$, which in turn implies

$$L = \sqrt{2N}. \quad (1.6)$$

In random matrix theory we recognise (1.5) and (1.6) as the Wigner semi-circle law for the eigenvalue density of large random real symmetric matrices; see e.g. [60]. This in fact is one of the derivations of the law given by Wigner himself [72].

Our interest in this paper is in analogies between eigenvalue PDFs with two-dimensional support in the complex plane, and the Boltzmann factor for one-component log-potential classical gases (plasmas) in two-dimensional domains. The meaning of the term one-component is that all charges are of the same sign and same strength, $+1$ say. The specific form of the logarithmic potential will depend on the surface defining the two-dimensional domain, e.g. a plane, sphere etc., and the particular boundary condition, which will be either free or Neumann. As already mentioned, (1.3) applies to planar geometry with free boundary conditions. Since the analogy holds at the level of the PDF, the corresponding correlations conserve this analogy, and so inherit properties characteristic of the plasma correlations.

The best known example of applicability of the analogy on the random matrix side is the ensemble of $N \times N$ standard complex Gaussian matrices, also referred to as complex Ginibre matrices [36]. Indeed it was Ginibre who first computed the joint eigenvalue PDF for this ensemble, showing it to be proportional to

$$\prod_{l=1}^N e^{-|z_l|^2} \prod_{1 \leq j < k \leq N} |z_k - z_j|^2, \quad z_l \in \mathbb{C}. \quad (1.7)$$

Writing this in the Boltzmann factor form $e^{-\beta U}$ shows

$$U = \frac{1}{2} \sum_{l=1}^N |z_l|^2 - \sum_{1 \leq j < k \leq N} \log |z_k - z_j| \quad (1.8)$$

with $\beta = 2$. The classical plasma system corresponding to (1.8) thus consists of N unit charges interacting via the pair potential (1.3), and a one-body two-dimensional harmonic potential towards the origin. The inverse temperature is $\beta = 2$. The one-body potential corresponds to the electrostatic potential created by a disk of uniform charge density $-1/\pi$ centred on the origin and of radius \sqrt{N} . To experience this potential the particles must be inside the disk; outside the disk the charge density is seen as a point charge of strength $-N$ at the origin, and the potential therefore becomes logarithmic. The analogy then breaks down, although according to the well known circle law (see e.g. [67]), to leading order all eigenvalues are in the disk of radius \sqrt{N} with uniform density $1/\pi$. Conversely, as a point to be emphasised in Section 2, the fact that a plasma system will to leading order be charge neutral (if it wasn't, there would be a nonzero electric field and the system would not be in equilibrium) predicts the circle law for the complex Ginibre matrices.

In Section 2 we review and extend other examples of the analogy and consequences for the global eigenvalue distribution. This involves three distinct geometries for the plasma — the plane, the sphere and the pseudosphere — and for each of these geometries three distinct random matrix ensembles depending on the entries being real, complex or real quaternion. Products of matrices from these ensembles are also considered from this viewpoint. In Section 3 we discuss consequences of the analogies with respect to general properties of the correlations known as sum rules. Sum rules considered relate to the moments of the truncated two-particle correlation, the decay of the correlations at the spectrum edge, and the vanishing of the complex moments of the screening cloud in the cases of fast decay of the two-particle correlation. The consideration of the latter leads us to exhibit an integral identity satisfied by the limiting two-particle correlation for real quaternion Ginibre matrices. Section 4 is devoted to providing further evidence to the proposal, due to Hastings [40], that with

$$\mathbb{Z}_{2N} := \mathbb{I}_N \otimes \begin{bmatrix} 0 & -1 \\ 1 & 0 \end{bmatrix}$$

and A_{2N} a complex anti-symmetric matrix with each independent element a standard complex Gaussian, the eigenvalues of the ensemble of random matrices of the form $\mathbb{Z}_{2N}A_{2N}$ are well described in the large distance regime by a joint PDF proportional to the form

$$\prod_{l=1}^N e^{-|z_l|^2} \prod_{1 \leq j < k \leq N} |z_k - z_j|^4, \quad z_l \in \mathbb{C}. \quad (1.9)$$

In the plasma analogy, the total potential is again given by (1.8) but with the pre-factor of the one-body term $\frac{1}{4}$ instead of $\frac{1}{2}$, while the inverse temperature is now $\beta = 4$. In Section 5, the eigenvalue PDF for single (quaternion) row and column deletion of circular symplectic ensemble matrices, recently computed explicitly in [49], is shown to have a plasma analogue. The latter is known in turn to be an example of a Pfaffian point process, and this enables the correlation functions for the eigenvalues to be computed, which in the $N \rightarrow \infty$ limit are identified as the eigenvalue correlations for random polynomials with standard complex Gaussian coefficients.

2 2d plasma analogies for some random matrix ensembles and consequences for the spectral density

Characteristic of the eigenvalue PDF for random matrix ensembles is the product of differences as seen in (1.1) and (1.7). Writing the PDF as the exponential of a potential energy, it is immediate that the corresponding pair potential represents a logarithmic repulsion between the eigenvalues, as seen from the viewpoint of a classical gas in equilibrium. A more sophisticated point, already known from the separate works [50], [28], is that the eigenvalue PDF for particular random matrix ensembles with support in the complex plane naturally projects to certain homogeneous manifolds — the sphere and the pseudosphere — where the eigenvalue density is uniform. Here we collect all these results together, give some extensions, and we make explicit the plasma prediction for the eigenvalue density. We remark that the theory of random polynomials, in which the coefficients are complex Gaussians with certain variances, also permits examples which have uniform density in the plane, on the sphere and on the pseudosphere [18, 39, 51].

The non-Hermitian random matrix ensembles in [50], [28] have complex entries. In these cases, as well as for the complex Ginibre ensemble, there is also an analogy with the absolute value squared of the wave function for N spinless fermions subject to a strong perpendicular magnetic field and in the lowest Landau level. This is discussed in e.g. [25, §15.2, §15.6, Ex. 15.7 q.2]. If we consider non-Hermitian random matrix ensemble with real or real quaternion elements the quantum mechanical analogy breaks down, whereas the plasma analogy persists, now with image charges due to Neumann boundary conditions. Again this point is known in scattered places in the literature, e.g. [25, §15.9.1] and [30] in the particular case of the Ginibre ensemble, but has not until now been the subject of a systematic investigation.

2.1 Ginibre ensembles

In keeping with Dyson's three fold way [16], there are three classes of Ginibre matrices, i.e. $N \times N$ Gaussian matrices with all elements independent and thus non-Hermitian. These classes are distinguished by the number field to which the elements belong — real, complex or real quaternion. In the latter case a 2×2 complex valued matrix representation is used; see e.g. [25, §1.3.2] and the eigenvalues occur in complex conjugate pairs. It has already been remarked that the joint eigenvalue PDF in the complex case is given by (1.1), and the analogy with a one-component plasma with neutralising background in a uniform disk of radius \sqrt{N} has been noted. Here we want to emphasise the reasoning which enables the leading order particle density of the plasma system, and thus the leading order eigenvalue density of the random matrix ensemble, to be determined.

The first step is to introduce a so-called global scaling of (1.7) by replacing $z_l \mapsto \sqrt{N}z_l$. A crucial feature of the product of differences in (1.7) is its scale invariance, changing by a multiplicative factor only. Introducing too the empirical density $\hat{\sigma}(z) := \sum_{p=1}^N \delta(z_p - z)$ shows that (1.7) is then proportional to

$$\exp\left(2\left\{-N \int_{\mathbb{C}} \hat{\sigma}(z)|z|^2 d^2z + \frac{1}{2} \int_{\mathbb{C} \times \mathbb{C} \setminus \{z=w\}} d^2z d^2w \hat{\sigma}(z)\hat{\sigma}(w) \log|z-w|\right\}\right). \quad (2.1)$$

We remark that the excluded set $z = w$ in the double integral in (2.1) corresponds, in physical terms, to the self energy of the charge density $\hat{\sigma}(z)$.

The essential physical idea, made rigorous using the theory of large deviations [7, 62] (see the discussion in the introduction to [65]) is that for large N the empirical density can be replaced by $N\rho^g(z)$, where $\rho^g(z)$ is the limiting global particle density normalised to have total integral equal to unity. Doing this, (2.1) reads

$$\exp\left(-2N^2\mathcal{E}[\rho(z)]\right), \quad \mathcal{E}[\rho(z)] := -\frac{1}{2} \int_{\mathbb{C}} \rho^g(z)|z|^2 d^2z + \frac{1}{2} \int_{\mathbb{C} \times \mathbb{C}} d^2z d^2w \rho^g(z)\rho^g(w) \log|z-w|. \quad (2.2)$$

Note that in this double integral there is no need to exclude the self energy term, as in contrast to (2.1) where it diverges, it makes a vanishingly small contribution. The final ingredient, which in idea is classical going back to at least Gauss (see e.g. [64]), is that the global density in (2.2) is such that the energy functional $\mathcal{E}[\rho(z)]$ is minimised. From the calculus of variations, this occurs when

$$0 = -\frac{1}{2}|z|^2 + \int_{\mathbb{C}} d^2w \rho^g(w) \log|z-w|. \quad (2.3)$$

But fundamentally $-\log|z-w|$ is the solution of the two-dimensional Poisson equation $\nabla_z^2 \phi(z, w) = -2\pi\delta^{(2)}(z-w)$ in free boundary condition, so acting on (2.3) with ∇^2 tells us that $\nabla^2|z|^2 = 2\pi\rho^g(z)$, for $z \in \mathcal{D}$. The region \mathcal{D} is referred to as the droplet (see e.g. [73]), and hence inside this region we have $\rho^g(z) = \frac{1}{\pi}$, while $\rho^g(z)$ vanishes outside \mathcal{D} . The last point to note is that to minimise $\mathcal{E}[\rho(z)]$, inspection of the functional form requires \mathcal{D} to be a disk about the origin, and the requirement that the integral of $\rho^g(z)$ over \mathcal{D} equals unity tells us that in fact \mathcal{D} is the unit disk. The unit disk is precisely the scaled limit of the uniform background charge density which gave rise to the Boltzmann factor (1.7) in the plasma interpretation.

Let's consider next the case of real quaternion elements. The eigenvalue PDF for the eigenvalues in the upper half complex plane is then proportional to [36], [57]

$$\prod_{j=1}^N e^{-2|z_j|^2} |z_j - \bar{z}_j|^2 \prod_{1 \leq j < k \leq N} |z_k - z_j|^2 |z_k - \bar{z}_j|^2. \quad (2.4)$$

A plasma analogy has previously been identified in [25, Prop. 15.9.1]. To review this result, the first point to note is that the solution of the two-dimensional Poisson equation $\nabla_{\vec{r}}^2 \phi(\vec{r}, \vec{r}') = -2\pi\delta(\vec{r} - \vec{r}')$ with the Neumann boundary condition along the x -axis

$$\frac{\partial}{\partial y} \phi(\vec{r}, \vec{r}') \Big|_{y \rightarrow 0^+} = 0, \quad (2.5)$$

is, using complex coordinates, given by

$$\phi(\vec{r}, \vec{r}') = -\log\left(|z - z'| |z - \bar{z}'|\right). \quad (2.6)$$

As discussed in [25, §15.9], this formally occurs when the region $y < 0$ has zero dielectric constant, which effectively gives rise to an image particle of identical charge at the reflection point \bar{z}' of z' about the real axis. We say formally, since physically a dielectric constant cannot be less than its vacuum value of unity. On the other hand, this circumstance is mimicked when the dielectric constant of the region $y > 0$ is much greater than the dielectric constant for $y < 0$.

Following [25, Prop. 15.9.1], consider now a one-component system — all particles of unit charge — confined to the semi-disk $|z| < \sqrt{N}$, $y > 0$, with a neutralising background of uniform density $\rho = 2/\pi$ filling the semi-disk. With the system interacting at the inverse temperature β , a short computation shows that the corresponding Boltzmann factor is proportional to

$$\prod_{j=1}^N e^{-\beta|z_j|^2} |z_j - \bar{z}_j|^{\beta/2} \prod_{1 \leq j < k \leq N} |z_k - z_j|^\beta |z_k - \bar{z}_j|^\beta. \quad (2.7)$$

In this expression, the origin of the term $\prod_{j=1}^N |z_j - \bar{z}_j|^{\beta/2}$ requires further explanation. The required theory is that the self-energy term in the total potential is computed according to the formula

$$\frac{1}{2} \sum_{j=1}^N \lim_{z' \rightarrow z_j} \left(\phi(z_j, z') - \log|z_j - z| \right) = -\frac{1}{2} \sum_{j=1}^N |z_j - \bar{z}_j|. \quad (2.8)$$

Note in particular the factor of $\frac{1}{2}$, which can be interpreted as saying the self energy is equally distributed between the actual and image system.

Comparing the eigenvalue PDF (2.4) and the Boltzmann factor (2.7) shows that for $\beta = 2$ they are identical, provided that in the Boltzmann factor an additional self-energy factor is included. Such a self-energy term is not expected to effect the large distance behaviours of the plasma, which instead are determined by the pair potential. Specific consequences by way of sum rules will be discussed in the next section. In this section the consequence of the plasma analogy that we emphasise is the implied eigenvalue density. By construction of the Boltzmann factor, the background charge density minimises the energy functional. Thus to leading order the eigenvalue density will be given by the background density, and so will be uniform in the semi-disk $|z| < \sqrt{N}$, $y > 0$.

The case of real Ginibre matrices is more complicated than for the complex or real quaternion Ginibre matrices. This is because in the real case there is a non-zero probability of some eigenvalues being real. Consequently the joint eigenvalue PDF consists of disjoint sectors depending of the number of real eigenvalues, k say (k must be of the same parity as N). In the upper half plane — note that all entries being real implies all the complex eigenvalues occur in complex conjugate pairs — the joint eigenvalue PDF, conditioned to have precisely k real eigenvalues $\{\lambda_l\}_{l=1, \dots, k}$, is proportional to [17]

$$\frac{1}{2^{N(N+1)/4} \prod_{l=1}^N \Gamma(l/2)} \frac{2^{(N-k)/2}}{k!((N-k)/2)!} \left| \Delta(\{\lambda_l\}_{l=1, \dots, k} \cup \{x_j \pm iy_j\}_{j=1, \dots, (N-k)/2}) \right| \\ \times e^{-\sum_{j=1}^k \lambda_j^2/2} e^{\sum_{j=1}^{(N-k)/2} (y_j^2 - x_j^2)} \prod_{j=1}^{(N-k)/2} \operatorname{erfc}(\sqrt{2}y_j), \quad (2.9)$$

where $\Delta(\{z_p\}_{p=1, \dots, m}) := \prod_{j < l}^m (z_l - z_j)$. Here $\lambda_l \in (-\infty, \infty)$ while $(x_j, y_j) \in \mathbb{R} \times \mathbb{R}_+$, $\mathbb{R}_+^2 := \{(x, y) \in \mathbb{R}^2 : y > 0\}$.

We can write

$$\begin{aligned}
& \left| \Delta(\{\lambda_l\}_{l=1,\dots,k} \cup \{x_j \pm iy_j\}_{j=1,\dots,(N-k)/2}) \right| \\
&= \exp\left(-\sum_{1 \leq j < p \leq k} \log |\lambda_p - \lambda_j| - \sum_{j=1}^k \sum_{s=k+1}^{(N+k)/2} \log |z_s - \lambda_j| |\bar{z}_s - \lambda_j| - \sum_{a,b=k+1}^{(N+k)/2} \log |z_a - \bar{z}_b|\right) \\
&\quad \times \exp\left(-\sum_{k+1 \leq a < b \leq (N+k)/2} \log |z_b - z_a| |\bar{z}_b - \bar{z}_a|\right). \quad (2.10)
\end{aligned}$$

A plasma interpretation of (2.10) has been discussed previously [30] in an analogous case (real spherical ensemble; see the next subsection). There the interpretation given was entirely in terms of the pair potential (1.3), with image charges imposed as a constraint. An alternative viewpoint is to consider instead the pair potential (2.6), with the charges on the real axis of strength $1/2$, at inverse temperature $\beta = 2$. Turning now to the one body term in (2.9), we first make the manipulation

$$e^{-\sum_{j=1}^k \lambda_j^2/2} e^{\sum_{j=1}^{(N-k)/2} (y_j^2 - x_j^2)} \prod_{j=1}^{(N-k)/2} \operatorname{erfc}(\sqrt{2}y_j) = e^{-\sum_{j=1}^k \lambda_j^2/2} e^{-\sum_{j=1}^{(N-k)/2} (x_j^2 + y_j^2)} \prod_{j=1}^{(N-k)/2} e^{2y_j^2} \operatorname{erfc}(\sqrt{2}y_j). \quad (2.11)$$

We see that the first two exponential terms on the RHS result from a coupling between the charges confined to the semi-disk $|z| < \sqrt{N}$, $y > 0$, and with a neutralising background of uniform density $\rho = 1/\pi$ filling the semi-disk (this is half the value of the corresponding background density in the real quaternion case due to there being of order $N/2$ rather than of order N eigenvalues in the semi-disk). The final term can be interpreted as the coupling to some external short range potential — note that to leading order it tends to unity as $y_j \rightarrow \infty$.

Analogous to the circumstance already mentioned in the case of the complex Ginibre ensemble, the neutralising background being the semi-disk $|z| < \sqrt{N}$, $y > 0$, implies that to leading order the particle density will also be uniform in this region. For the real Ginibre ensemble, the eigenvalues not on the real axis occur in complex conjugate pairs, so the corresponding eigenvalue density is to leading order anticipated to be uniform in the disk $|z| < \sqrt{N}$ in keeping with the circle law. Note in particular that the real eigenvalues play no role in this leading order statement, as their proportion is on average $1/\sqrt{N}$ [17], and is thus vanishingly small as $N \rightarrow \infty$.

Let G be from a Ginibre ensemble (real, complex or real quaternion entries), and construct the matrix [66]

$$Y = \frac{1 + \sqrt{c}}{2} G + \frac{1 - \sqrt{c}}{2} G^\dagger, \quad c = \frac{1 - \tau}{1 + \tau} \quad (0 \leq \tau < 1). \quad (2.12)$$

The eigenvalue PDF of this deformation of the Ginibre ensemble was analysed in [52] in the real case, in [34] in the complex case, and in [47] in the real quaternion case. In each case, the only modification to the eigenvalue PDF relative to that for the case $c = 1$, i.e. the original Ginibre ensemble, occurs in the one-body factors. Specifically, in the complex and real quaternion cases, replace

$$e^{-\sum_{j=1}^N |z_j|^2} \mapsto \exp\left(-\frac{1}{1 - \tau^2} \sum_{j=1}^N \left(|z_j|^2 - \frac{\tau}{2}(z_j^2 + \bar{z}_j^2)\right)\right), \quad (2.13)$$

while in the real case (2.10), replace

$$\prod_{j=1}^{(N-k)/2} \operatorname{erfc}(\sqrt{2}y_j) \mapsto \prod_{j=1}^{(N-k)/2} \operatorname{erfc}\left(\frac{\sqrt{2}}{1 - \tau} y_j\right),$$

up to the normalisation. In the real case, substituting in (2.10) and replacing the complimentary error function by its leading asymptotic form reclaims the RHS of (2.13) for the functional form of the one-body factor for the complex eigenvalues.

Thus, from the viewpoint of the present theme, our task is to interpret the RHS of (2.13) as a coupling of a background charge density to the mobile charges of the plasma. Actually, the answer to this is already known [27, 33]; see also [25, Ex. 15.2 q.4]. We have that the RHS of (2.13) results from a uniformly charged ellipse, charge density $-1/\pi(1-\tau^2)$, with semi-axes $A = \sqrt{N}(1+\tau)$, $B = \sqrt{N}(1-\tau)$. Note that this is consistent with the elliptic law in random matrix theory (see e.g. [58]) as a generalisation of the circular law.

2.2 Spherical ensembles

Following [50], as motivation for the study of the spherical ensembles as a natural next step from the study of the Ginibre ensembles, take two Ginibre matrices G_1 and G_2 , both with entries from the same number field and consider the generalised eigenvalue problem $G_1\vec{v} = \lambda G_2\vec{v}$. The generalised eigenvalues λ are the eigenvalues of the random matrix product $G_2^{-1}G_1$, and it is eigenvalues of this type of matrix that make up the spherical ensemble.

The naming can be justified by relating the eigenvalue distribution of $G_2^{-1}G_1$ to the geometry of the sphere. Further following [50], for this purpose we specialise to the complex case, and introduce the transformed pair of matrices (C, D) according to

$$C := -\bar{\beta}G_2 + \bar{\alpha}G_1, \quad D = \alpha G_2 + \beta G_1,$$

with $\alpha, \beta \in \mathbb{C}$ and such that

$$|\alpha|^2 + |\beta|^2 = 1. \quad (2.14)$$

One can check that (G_1, G_2) has the same distribution as (C, D) . From this latter fact one can check that the distribution of the generalised eigenvalues is unchanged by the fractional linear transformation

$$\lambda \mapsto \frac{\lambda\alpha - \bar{\beta}}{\lambda\beta - \bar{\alpha}}. \quad (2.15)$$

This combined with (2.14) implies that upon a stereographic projection from the complex plane to the Riemann sphere the eigenvalue distribution of $G_2^{-1}G_1$ is invariant under rotation of the sphere, and thus the name of the ensemble.

The plasma analogy is very direct in the complex case. Thus in this case the joint eigenvalue PDF is proportional to [50]

$$\prod_{l=1}^N \frac{1}{(1+|z_l|^2)^{N+1}} \prod_{1 \leq j < k \leq N} |z_k - z_j|^2, \quad z_l \in \mathbb{C}. \quad (2.16)$$

As noted in e.g. [25, §15.6.4], a stereographic projection from the Riemann sphere of radius $\frac{1}{2}$ to the complex plane, located tangent to the north pole, is specified by the equation

$$z = e^{i\phi} \tan \frac{\theta}{2}. \quad (2.17)$$

Making this change of variables transforms (2.16) to the PDF on the sphere proportional to

$$\prod_{1 \leq j < k \leq N} |\vec{r}_k - \vec{r}_j|^2, \quad (2.18)$$

where \vec{r}_j is the vector in \mathbb{R}^3 corresponding to the point (θ_j, ϕ_j) on the sphere.

To compare (2.18) to the Boltzmann factor for a one-component plasma on a sphere, the first point to note is that in this geometry the solution of the charge neutral Poisson equation

$$\nabla_{\theta, \phi}^2 \phi((\theta, \phi), (\theta', \phi')) = -2\pi\delta_S((\theta, \phi), (\theta', \phi')) + \frac{1}{2R^2} \quad (2.19)$$

(charge neutrality is a necessary condition for the existence of a solution, due to the sphere being a compact surface), where $\delta_S((\theta, \phi), (\theta', \phi'))$ is the Dirac delta function on the sphere and R is the radius, is given by

$$-\log |\vec{r} - \vec{r}'|, \quad (2.20)$$

where \vec{r}, \vec{r}' are the points in \mathbb{R}^3 corresponding to $(\theta, \phi), (\theta', \phi')$ on the sphere. Hence for N unit charges on the sphere, in the presence of a uniform background, and at inverse temperature $\beta = 2$, the Boltzmann factor is precisely (2.18) [11]. The uniform background of the plasma is consistent with the uniform eigenvalue density when projected on the sphere, as follows from the invariance (2.15).

In the case of the real quaternion spherical ensemble, the joint eigenvalue PDF in the complex plane is proportional to [56]

$$\prod_{j=1}^N \frac{|\lambda_j - \bar{\lambda}_j|^2}{(1 + |\lambda_j|^2)^{2(N+1)}} \prod_{1 \leq j < k \leq N} |\lambda_k - \lambda_j|^2 |\lambda_k - \bar{\lambda}_j|^2, \quad \lambda_j \in \mathbb{C}_+. \quad (2.21)$$

Upon stereographic projection, this maps to the PDF on the half sphere \mathbb{S}_+^2 , the latter defined by the restriction on the azimuthal angle $0 \leq \phi \leq \pi$, proportional to

$$\prod_{j=1}^N |\vec{r}_j - \vec{r}_j^*|^2 \prod_{1 \leq j < k \leq N} |\vec{r}_k - \vec{r}_j|^2 |\vec{r}_k - \vec{r}_j^*|^2, \quad \vec{r}_j \in \mathbb{S}_+^2, \quad (2.22)$$

where \vec{r}_j^* is the vector in \mathbb{R}^3 corresponding to the point on the sphere $(\theta_j, -\phi_j)$. The plasma interpretation is the sphere analogue of that for the real quaternion Ginibre eigenvalue PDF (2.4). Thus one considers N unit charges confined to the half sphere \mathbb{S}_+^2 , with Neumann boundary conditions at the boundary, for which the potential at \vec{r}_b due to a charge at \vec{r}_a is

$$-\log \left(|\vec{r}_b - \vec{r}_a| |\vec{r}_b - \vec{r}_a^*| \right), \quad (2.23)$$

and in the presence of a neutralising background. At the coupling $\beta = 2$ the corresponding Boltzmann factor is (2.22), except that in (2.22) there is an additional one-body factor $\prod_{j=1}^N |\vec{r}_j - \vec{r}_j^*|$. The background being uniform is the plasma mechanism for the eigenvalue density also being uniform to leading order as $N \rightarrow \infty$ [55].

The real spherical ensemble shares with the real Ginibre ensemble the property of having real eigenvalues, in addition to eigenvalues occurring in complex conjugate pairs, and the joint eigenvalue PDF correspondingly breaks up into sectors analogous to (2.9). The functional form of the one-body terms are at first complicated [30, Eqns. (21) and (22)], but simplify upon a fractional linear transformation mapping the upper half plane to the unit disk [30, Eqns. (6) and (7)]. Then mapping the unit disk to the upper half of the Riemann sphere $0 < \theta < \pi/2$ via a stereographic projection with the complex plane passing through the sphere at the equator, we see that the effective pair potential for the complex eigenvalues is again (2.23), but now with \vec{r}^* obtained from \vec{r} by mapping the polar angle $\theta \mapsto \pi - \theta$. The real eigenvalues are their own images, and to account for this it is necessary that they be chosen to have charge 1/2 rather than unity as for the complex eigenvalues. Some one-body terms remain, but they are independent of N , and so are not expected to alter large distance properties of the plasma. In particular there being a uniform neutralising background tells us that to leading order in N the eigenvalue density will be uniform when projected on the sphere, which is indeed the case [11, 30]. As for the real Ginibre ensemble, the fact that there are real eigenvalues does not effect this property.

2.3 Truncated unitary ensembles

The eigenvalue distribution in the complex plane for sub-matrices of unitary matrices was first considered by Życzkowski and Sommers [74]. The setting is to choose a matrix from the set of $(N + n) \times (N + n)$ unitary matrices $U(N + n)$ under the assumption of Haar measure, then to delete n rows and n columns

to form an $N \times N$ sub-matrix. The point of interest is the corresponding eigenvalue PDF, which was shown in [74] to be proportional to

$$\prod_{l=1}^N (1 - |z_l|^2)^{n-1} \chi_{|z_l| < 1} \prod_{1 \leq j < k \leq N} |z_k - z_j|^2, \quad (2.24)$$

where $\chi_A = 1$ for A true and $\chi_A = 0$ otherwise. The plasma analogy was identified in [28], and now relates not to the sphere but to the pseudosphere, which is a two-dimensional hyperbolic space with constant negative Gaussian curvature $\kappa = -1/a^2$. It is naturally embedded in three-dimensional Minkowski space, with co-ordinates (y_0, y_1, y_2) and line element such that $(ds)^2 = -(dy_0)^2 + (dy_1)^2 + (dy_2)^2$. Specifically, the pseudosphere is the branch of the solution of the equation $-y_0^2 + y_1^2 + y_2^2 = -a^2$ which includes the point $(a, 0, 0)$. This branch can be parameterised by

$$y_0 = a \cos \tau, \quad y_1 = a \sinh \tau \cos \phi, \quad y_2 = a \sinh \tau \sin \phi. \quad (2.25)$$

With $z = x + iy$, the pseudosphere is projected onto the Poincaré disk via the stereographic projection (as interpreted in Euclidean space)

$$z = 2a \tanh \frac{\tau}{2} e^{i\phi}, \quad |z| < 2a, \quad (2.26)$$

(we will take $a = 1/2$) or equivalently by the polar form $z = r e^{i\phi}$ with $r = 2a \tanh \frac{\tau}{2}$. Note that this is identical to (2.17), if we set $\tau = i\theta$, $a = iR$, where R is the radius of the sphere (in (2.17), $R = 1/2$), thus justifying the name pseudosphere. It turns out that this same prescription applies to deducing the solution of the Poisson equation on the pseudosphere from knowledge of the solution of (2.19), giving the pair potential (see e.g. [44])

$$-\log \left(\frac{|z_j - z_k|}{(1 - r_j^2)^{1/2} (1 - r_k^2)^{1/2}} \right). \quad (2.27)$$

A significant difference between the pseudosphere and the sphere is that the former is not compact, and so does not require charge neutrality on the RHS of the Poisson equation for a solution. This is just as well, since setting $R = ia$ in (2.19) implies that the smeared out background is of the same sign as the mobile charges, with charge density $1/4\pi a^2$. With N particles, the total charge density is $N/4\pi a^2$, so to get a net background charge density $-\eta$ we must cancel this and impose a smeared out charge density $-\eta - N/4\pi a^2$. A short computation [44] gives that for $\beta = 2$ and $a = 1/2$, and using the variables (2.26), the corresponding Boltzmann factor is proportional to

$$\prod_{j=1}^N (1 - |z_j|^2)^{\pi\eta+1} \chi_{|z_j| < 1} \prod_{1 \leq j < k \leq N} |z_k - z_j|^2, \quad (2.28)$$

and hence is the same functional form as the PDF (2.24) with

$$n = \pi\eta + 2. \quad (2.29)$$

We can use the plasma analogy to predict the leading order large N form of the eigenvalue density, in the case that $n/N \rightarrow c > 0$. On the pseudosphere the neutralising background has constant charge density $-\eta$, and we have $\eta \approx n/\pi$ for n large. We know too (see e.g. [25, Eq. (15.161)]) that the pseudosphere surface element dS projects to the Poincaré disk according to

$$dS = \frac{dx dy}{(1 - |z|^2)^2}. \quad (2.30)$$

The total number of particles in a disk of radius R within the Poincaré disk is thus $\pi\eta R^2/(1 - R^2)$. Substituting for η and equating this to N allows us to specify R , and we conclude that the leading order eigenvalue density will be given by

$$\frac{n + N}{\pi(1 - |z|^2)^2} \chi_{|z| < R}, \quad R = \left(\frac{1}{1 + n/N} \right)^{1/2}, \quad (2.31)$$

in agreement with the result of an explicit analysis of the one-point density [35].

We now turn our attention to the case of truncations of unitary matrices with real quaternion elements. Such matrices are equivalent to unitary symplectic matrices, and so make up one of the classical groups, denoted $\text{Sp}(2m)$ for matrices of size $m \times m$ (the $2m$ in $\text{Sp}(2m)$ refers to the row or column size of the corresponding complex matrix — recall each real quaternion is represented as a 2×2 matrix). We suppose that the original matrices are of size $(N + n) \times (N + n)$, and consider sub-blocks of size $N \times N$. The corresponding eigenvalue PDF has been reported in the recent work [42], although no details as to its derivation were given. As a possible strategy, we begin by noting from [24, $N \mapsto N + n, n_1 = n_2 = N, \beta = 4$] that the distribution of an $N \times N$ sub-block A say is proportional to

$$\det(\mathbb{I}_N - A^\dagger A)^{2(n-N+1/2)}. \quad (2.32)$$

Note that this requires $n \geq N$ to be well defined; if not some eigenvalues of $A^\dagger A$ are unity, and the distribution of A is singular.

Next we note that the distribution (2.32) is analogous to the distribution

$$\det(\mathbb{I}_N + A^\dagger A)^{-2(n+N)} \quad (2.33)$$

for matrices $A = (B^\dagger B)^{-1/2} X$, with B, X given by $n \times n$ ($n \times N$) real quaternion matrices respectively, for which Mays [55, 56] has computed the joint eigenvalue PDF as proportional to (2.21) but with the replacement

$$1/(1 + |\lambda_j|^2)^{2(N+1)} \mapsto 1/(1 + |\lambda_j|^2)^{2(n+1)}. \quad (2.34)$$

The significance of this is that, as first demonstrated in the complex case, and used subsequently in the real case [55], the working required to deduce the joint eigenvalue PDF starting with a spherical ensemble density such as (2.33) is structurally identical to that required for the same task as starting with the PDF (2.32). The final results must be the same except that the parameter n is to be replaced by $-(n + 1/2)$ as is consistent in going from (2.33) to (2.32), and the factors $(1 + |\lambda_j|^2)$ must be replaced by $(1 - |\lambda_j|^2)$ for the same reason. Hence, from knowledge of the eigenvalue PDF corresponding to (2.33) being given by (2.21) with the replacement (2.34), it must be that the eigenvalue PDF corresponding to the distribution (2.32) on random matrices with real quaternion entries is proportional to

$$\prod_{l=1}^N (1 - |z_l|^2)^{2n-1} |z_l - \bar{z}_l|^2 \prod_{1 \leq j < k \leq N} |z_k - z_j|^2 |z_k - \bar{z}_j|^2, \quad |z_l| < 1, \quad (2.35)$$

in agreement with the functional form reported in [42]. As in the complex case [28], even though our derivation of (2.35) has required $n \geq N$ due to it being based on (2.32), the final expression is well defined for all $n \geq 1$ and is expected to be generally true (in the complex case this can be checked by an alternative derivation [74]).

For the plasma analogy, we consider a half pseudosphere, specified by (2.25) with $0 \leq \phi \leq \pi$ and impose Neumann boundary conditions at $\phi = 0, \pi$. The corresponding pair potential is then

$$-\log \left(\frac{|z_j - z_k| |z_j - \bar{z}_k|}{(1 - r_j^2)(1 - r_k^2)} \right) \quad (2.36)$$

(cf. (2.27)). Recalling that the solution (2.36) corresponds to setting $R = ia$ in (2.19), and thus each charge effectively contributes uniform smeared out background of charge density $1/4\pi a^2$, we see that we must impose a smeared out background charge density $-2(\eta + N/4\pi a^2)$ on the half pseudosphere. As noted in [44], a one-body potential $V(r)$ satisfying

$$\nabla^2 V = 4\pi(\eta + N/4\pi a^2)$$

is then created, where ∇^2 is the appropriate Laplacian operator on the pseudosphere. This has solution

$$V(r) = -(4\pi\eta a^2 + N) \log \left(1 - \frac{r^2}{4a^2} \right),$$

and the total potential energy due to the coupling between the background and the particles is then $\sum_{j=1}^N V(r_j)$. Adding to this the potential energy due to the particle-particle interaction as calculated from the pair potential (2.36), and the self energy terms as calculated using the LHS of (2.8), we see that the Boltzmann factor is proportional to

$$\prod_{j=1}^N (1 - |z_j|^2)^{2\pi\eta+1} |z_j - \bar{z}_j|^{\chi_{|z_j|<1}} \prod_{1 \leq j < k \leq N} |z_k - z_j|^2 |z_k - \bar{z}_j|^2. \quad (2.37)$$

As in common with (2.4) and (2.22), the eigenvalue PDF (2.35) contains an extra factor of the term in (2.37) corresponding to the self-image. Also, the identification (2.29) must now be modified to read

$$n = \pi\eta + 1. \quad (2.38)$$

With these points noted, we thus have an analogy between the eigenvalue PDF for truncations of random unitary matrices with real quaternion elements, and the Boltzmann factor of the one-component plasma on the half pseudosphere with Neumann boundary conditions. As in the complex case, an immediate consequence, due to the background being uniform, is the formula (2.31) for the predicted leading order eigenvalue density in the case that $n, N \rightarrow \infty$ with n/N fixed.

The final case to consider relating to truncations is when the elements of the unitary matrix are real, and so the matrices a real orthogonal, which like $\text{Sp}(2m)$ make up one the classical groups, the orthogonal group denoted $O(m)$ for matrices of size $m \times m$. It is shown in [48] that the joint eigenvalue PDF, which due to there being real eigenvalues breaks up into sectors depending on the number of real eigenvalues, is structurally identical to (2.9) but with the one body factors (2.11) replaced by $\prod_{l=1}^k w_r(\lambda_l) \prod_{s=1}^{(N-k)/2} w_c(x_s, y_s)$, where with $z = x + iy$,

$$w_r(\lambda) \propto (1 - \lambda^2)^{n/2-1}, \quad w_c(x, y) \propto |1 - z^2|^{n-2} \left(|1 - z^2|^{n/2-1} \int_{2y/|1-z^2|}^1 (1 - t^2)^{(n-3)/2} dt \right)^2. \quad (2.39)$$

We have discussed the plasma interpretation of the two body factors in (2.9), which are thus the same in the present setting. For the one-body terms, we note that the factor in $w_c(x, y)$ in large brackets is of order unity as $|z| \rightarrow 1$ and so can be considered as a coupling to a short range potential, as with the final term in (2.11), whereas the first factor in $w_c(x, y)$ and the expression for $w_r(\lambda)$ each result from a coupling between a neutralising background $-(\eta + N/4\pi a^2)$ on the half pseudosphere, and the pair potential (2.36) for a unit and half unit charge respectively. A precise relation between η and n as in (2.29) and (2.38) cannot be made due to the arbitrariness of the factorisation of $w_c(x, y)$. But for large n we must have $n \approx \pi\eta$ and this implies the validity of the plasma analogy prediction of the spectral density again being given by (2.31), in the appropriate limit.

2.4 Induced ensembles

Let G be an $N \times N$ random matrix with real, complex or real quaternion elements, and let U be a unitary matrix with elements from the same number field. With

$$A = (G^\dagger G)^{1/2} U, \quad (2.40)$$

it follows that $A^\dagger A$ and $G^\dagger G$ have the same matrix distribution, and in particular that $A^\dagger A$ and $G^\dagger G$ have the same distribution of singular values. Suppose that in addition the distribution of G is unchanged by left or right multiplication by a unitary matrix. Since by the singular value decomposition, for some unitary matrices U_1, U_2 we have $G = U_1 \Sigma U_2$, where Σ is a diagonal matrix of the singular values, by this last assumption G has the same distribution as $U \Sigma$, where U is chosen with Haar measure. Substituting this in the definition of A tells us that A has the same distribution as ΣU , but this is also distributed as G , so we come to the conclusion that A and G are equal in distribution, and so have the same distribution of eigenvalues. Note in particular that the Ginibre, spherical and truncated unitary ensembles all have

their elements G unchanged in distribution by left or right multiplication by a unitary matrix, and so this statement applies to those cases.

The construction (2.40) is well defined for G rectangular of size $n \times N$ say. Given that G is from a random matrix ensemble, a relevant question to ask is how the volume element of G , (dG) , is related to (dA) . Following [20], to answer this question we begin by considering $C := G^\dagger G$. With $n \geq N$, it is a standard result (see e.g. [25, Eq. (3.30)]) that

$$(dG) \propto (\det C)^{(\beta/2)(n-N-1+2/\beta)}(dC), \quad (2.41)$$

where $\beta = 1, 2, 4$ according to the entries of G being real, complex or quaternion real. Suppose also that the distribution of G is unchanged by multiplication by a unitary matrix on the right. We then have

$$A^\dagger A = U^\dagger G^\dagger G U \stackrel{d}{=} G^\dagger G = C,$$

where the equality in distribution follows by the assumption of the appropriate invariance of the distribution of G . From this, and noting A is of size $N \times N$, the analogue of (2.41) reads

$$(dA) \propto (\det C)^{(\beta/2)(-1+2/\beta)}(dC). \quad (2.42)$$

Comparing (2.41) and (2.42) we conclude

$$(dG) \propto (\det A^\dagger A)^{(\beta/2)(n-N)}(dA). \quad (2.43)$$

As noted in [22], a corollary is that if the distribution of G is

$$g(G^\dagger G), \quad (2.44)$$

with G unitary invariant, then A has distribution proportional to

$$(\det A^\dagger A)^{(\beta/2)(n-N)}g(A^\dagger A). \quad (2.45)$$

And it follows from this that if the eigenvalue PDF for matrices G distributed as $g(G^\dagger G)$ is given by $f(\lambda_1, \dots, \lambda_N)$, then in the rectangular case with the construction (2.40), the eigenvalue PDF is proportional to

$$\prod_{l=1}^N |z_l|^{\beta(n-N)} f(z_1, \dots, z_N). \quad (2.46)$$

The assumptions on G leading to (2.45), specifically the form (2.44) and its unitary invariance, hold for rectangular analogues of each of the Ginibre, spherical and truncated unitary ensembles. Each has three sub-cases, depending on the elements being real ($\beta = 1$), complex ($\beta = 2$) or real quaternion ($\beta = 4$). In the Ginibre case, we take G in (2.40) to be an $n \times N$ standard Gaussian matrix. The distribution on G is then proportional to $e^{-(\beta/2)\text{Tr} G^\dagger G}$. In the spherical case we take $G = G_1^{-1} G_2$ where G_1 (G_2) is an $n \times n$ ($n \times N$) standard Gaussian matrix. The joint density of G is then proportional to [25, Ex. 3.6 q.3]

$$\det(\mathbb{I}_N + G^\dagger G)^{-(\beta/2)(n+N)}. \quad (2.47)$$

In the case of truncated unitary matrices we begin with a unitary matrix of size $M \times M$ and then select a sub-block of size $n \times N$ which we call G . For $M - (n + N) \geq 0$ we know [24] that the joint distribution of G is proportional to

$$\det(\mathbb{I}_N - G^\dagger G)^{(\beta/2)(M-(n+N)+1-2/\beta)}. \quad (2.48)$$

Note that (2.47) and (2.48) reduce to (2.32) and (2.33) with $\beta = 4$, after allowing for differences in notation.

In all these cases the eigenvalue PDF will have the structure (2.46). Consider for definiteness the rectangular Ginibre ensembles. The factor

$$\prod_{l=1}^N |z_l|^{\beta(n-N)} = \prod_{l=1}^N e^{\beta(n-N) \log |z_l|} \quad (2.49)$$

has the immediate plasma interpretation of a repulsion from the origin by a charge of strength $(n - N)$. However this interpretation is not informative from a random matrix viewpoint as it does not allow us to read off the eigenvalue density. Another interpretation is therefore called for. We make use of Newton's theorem, which tells us that the potential created by a point charge is the same as that created by a spherically symmetric continuous smeared out charge density when viewed from the outside of the latter.

Newton's theorem permits the interpretation of (2.49) as due to a smeared out uniform charge density $1/\pi$ confined to a radius $\sqrt{n - N}$ about the origin, with the plasma particles confined to lie outside this region. On the other hand, we know that the factor $e^{-\beta|z_i|^2/2}$ results from a smeared out charge density $-1/\pi$ when viewed from inside the plasma. These charge densities therefore cancel in the region $|z| < \sqrt{n - N}$. For charge neutrality the outer radius must now extend to \sqrt{n} , so the total background charge density is equal to $-1/\pi$ in the annulus

$$\sqrt{n - N} < |z| < \sqrt{n} \quad (2.50)$$

and is zero elsewhere. This particular plasma interpretation gives an immediate prediction for the eigenvalue density: to leading order it will be uniform in the annulus (2.50) with density $1/\pi$. This is in keeping with the result from asymptotic analysis of the analytic form for the eigenvalue density [22], and provides an explicit example of the so-called single ring theorem [19].

The factor (2.49) can be similarly interpreted in the spherical and truncated unitary ensembles, although there is an added complication of f in (2.46) now also depending on n . For ease of presentation we will restrict attention to the case of complex elements. Actually the plasma analogy for the complex spherical ensemble has been discussed previously [21].

The first point to note is that substitution of (2.47) in (2.29) shows that for the spherical ensemble the matrices A as specified by (2.40) have distribution proportional to

$$(\det A^\dagger A)^{(\beta/2)(n-N)} \det(\mathbb{I}_N + A^\dagger A)^{-(\beta/2)(n+N)}.$$

In the case $\beta = 2$ (complex elements) this implies the joint eigenvalue PDF [21, $N \mapsto n, M \mapsto N, n \mapsto N$] proportional to

$$\prod_{j=1}^N \frac{|z_j|^{2(n-N)}}{(1 + |z_j|^2)^{n+1}} \prod_{1 \leq j < k \leq N} |z_k - z_j|^2 \quad (2.51)$$

(note that this reduces to (2.16) in the case $n = N$). Upon stereographic projection (2.17) this takes on the form

$$\prod_{l=1}^N |\vec{r}_l|^{2(n-N)} \prod_{1 \leq j < k \leq N} |\vec{r}_k - \vec{r}_j|^2, \quad (2.52)$$

where as in (2.18) \vec{r}_j is the vector in \mathbb{R}^3 corresponding to the point (θ_j, ϕ_j) on the sphere, with the origin at the north pole.

We seek a one-component plasma system on the sphere with a uniform background charge that has Boltzmann factor (2.52). An important point is that on the sphere each charge is accompanied by a neutralising smeared out uniform charge density (recall (2.19)). This means that if we consider a spherical cap about the north pole specified by $0 < \theta < \theta^*$, of area $A_{\theta^*} = \frac{\pi}{2}(1 - \cos \theta^*)$, then the uniform charge density in that region is $-NA_{\theta^*}/\pi$. We want to impose an external uniform charge density A_{θ^*}/π in $\theta^* < \theta < \pi$, which furthermore will be the region occupied by the mobile charges. Doing this, and choosing

$$\frac{A_{\theta^*}}{\pi} = \frac{n/N - 1}{n/N}, \quad (2.53)$$

it is shown in [21] that (2.52) is, up to a multiplicative constant, the Boltzmann factor for the plasma system. Note that this predicts that the eigenvalue density will to leading order be supported on the portion of the sphere specified by the azimuthal angle being in the range $\theta^* < \theta < \pi$, and will be uniform. We remark too that in the complex plane, the formula (2.53) and the stereographic projection formula

(2.17) tell us that the inner boundary of support r^* say satisfies $(r^*)^2 = \frac{n}{N} - 1$ [21], while the density profile in this support is

$$\frac{n}{\pi(1 + |z|^2)}. \quad (2.54)$$

It remains to identify the plasma system for rectangular truncated unitary matrices subject to the construction (2.40). Here, from the discussion in the paragraph below (2.46), and (2.29), the matrices A as specified by (2.40) have distribution proportional to

$$(\det A^\dagger A)^{(\beta/2)(n-N)} \det(\mathbb{I}_N - A^\dagger A)^{(\beta/2)(M-(n+N)+1-2/\beta)}.$$

The corresponding joint eigenvalue PDF is known to be proportional to [22]

$$\prod_{j=1}^N \left(\frac{|z_j|^2}{1 - |z_j|^2} \right)^{n-N} (1 - |z_j|^2)^{M-N-1} \prod_{1 \leq j < k \leq N} |z_k - z_j|^2 \quad (2.55)$$

(note that this gives (2.24) in the case $n = N$ and $M \mapsto N + n$). To relate this to the Boltzmann factor for a plasma system, we proceed as for the task of similarly interpreting (2.24).

First, a smeared out neutralising charge density $-(\eta + N/4\pi a^2)$ is to be imposed on the pseudosphere, and we set $a = 1/2$. We know that for the corresponding one-component plasma system (2.28) is proportional to the Boltzmann factor. Next, for $\tau > \tau_-$ the potential, by Newton's theorem, will be that of a charge at the origin of strength

$$Q = A_{\tau_-} (\eta + N/4\pi a^2), \quad (2.56)$$

where $A_{\tau_-} = 2\pi a^2 (\cosh \tau_- - 1)$ is the area of the region $0 < \tau < \tau_-$. According to (2.36), this potential is therefore equal to $-Q \log(|z|/(1 - |z|^2)^{1/2})$, and so with the particles confined to the region $\tau > \tau_-$ the Boltzmann factor is given by (2.28) multiplied by $\prod_{j=1}^N (|z_j|^2/(1 - |z_j|^2))^Q$, giving us in total the functional form (2.55) with

$$Q = n - N \quad (2.57)$$

and $\pi\eta + 1 = M - N - 1$. Let us suppose R_- is related to τ_- by stereographic projection. Noting from (2.30) that the area on the pseudosphere with $a = 1/2$, corresponding to a disk of radius R_- in the complex plane centred on the origin, is equal to $\pi R_-^2/(1 - R_-^2)$, we then we have from (2.56) that $Q = (M - 2)R_-^2/(1 - R_-^2)$, and this equated with (2.57) tells us that for large n, M, N ,

$$R_-^2 = \frac{(n - N)/M}{1 + (n - N)/M}. \quad (2.58)$$

The outer radius R_+ of the support of the eigenvalue density can similarly be computed. Since the background charge in $|z| < R_-$ is $-Q = -(n - N)$ and this has been neutralised, we require that the total charge for $|z| < R_+$ be equal to $N + Q = n$ so has to have total charge in $R_- < |z| < R_+$ equal to N . Recalling too from below (2.57) that for large $M - N$, $\pi\eta \approx M - n$ we obtain

$$R_+^2 = \frac{1}{1 + (M - N)/n}. \quad (2.59)$$

Note that this is consistent with (2.31) once we make the identification noted below (2.55). These formulas are in agreement with the exact results reported in [22].

2.5 Products of random matrices

Consider the product of m independent Ginibre matrices. Considerations from free probability [9], [38], [59] tell us that

$$\lim_{N \rightarrow \infty} \frac{1}{N} N^m \rho_{(1)}(N^{m/2} w) = \frac{|w|^{(2/m)-2}}{m\pi} \chi(|w| < 1). \quad (2.60)$$

Let us suppose the Ginibre matrices have complex elements. A recent advance in random matrix theory has been the exact determination of the joint eigenvalue PDF [2], which has been shown to be proportional to

$$\prod_{l=1}^N w_m^{(2)}(|z_l|) \prod_{1 \leq j < k \leq N} |z_k - z_j|^2, \quad w_m^{(2)}(|z|) = G_{0,m}^{m,0} \left(\begin{matrix} - \\ 0, \dots, 0 \end{matrix} \middle| |z|^2 \right). \quad (2.61)$$

Here $G_{0,m}^{m,0}$ is an example of the Meijer G-function; see e.g. [53]. From a plasma viewpoint, we can replace $w_m^{(2)}(|z|)$ by its large $|z|$ form,

$$w_m^{(2)}(|z|) \underset{|z| \rightarrow \infty}{\sim} e^{-m|z|^{2/m} + O(\log |z|)} \quad (2.62)$$

obtained from known asymptotics of the Meijer G-function [53]. Substituting this in (2.61), and going through the argument below (2.2), we see that the plasma viewpoint correctly predicts (2.60).

Note that changing variables $|w| = r^m$ in (2.60) reclaims the circle law. An understanding of this observation has been given in [10], as a corollary of the fact that the limiting global spectral density of a product of m Ginibre matrices is equal to that for a single Ginibre matrix raised to the m -th power. The mechanism for this — that Ginibre matrices are unchanged in distribution by multiplication on the left or right by unitary matrices in the same number field — also holds true for the spherical ensemble and truncations of unitary matrices.

Thus for a product of m independent $N \times N$ matrices from the spherical ensemble, changing variables $|z| = |w|^{1/m}$ in the stereographic projection of the uniform density on the sphere of radius $1/2$,

$$\frac{1}{\pi(1 + |z|^2)^2}$$

(cf. (2.54)) gives the asymptotic density [37]

$$\frac{N|w|^{2/m-2}}{\pi m(1 + |w|^{2/m})^2}. \quad (2.63)$$

Similarly, the same change of variables in (2.31) gives, for the product of m independent truncations of $U(n + N)$ matrices of size $N \times N$, the asymptotic density [10]

$$\frac{(n + N)w^{2/m-2}}{\pi m(1 - |w|^{2/m})^2} \chi_{|w| < R^m}, \quad (2.64)$$

where R is given in (2.31).

To understand (2.63) and (2.64) from a plasma viewpoint, we first note from [1] and [3] (see also the review [4]) that in the case of complex entries the eigenvalue PDF for products of m spherical ensemble matrices, or m truncated unitary matrices, is again of the form (2.61), but with $w_m(|z|)$ replaced by

$$G_{m,m}^{m,m} \left(\begin{matrix} -N, \dots, -N \\ 0, \dots, 0 \end{matrix} \middle| |z|^2 \right), \quad G_{m,m}^{m,0} \left(\begin{matrix} n, \dots, n \\ 0, \dots, 0 \end{matrix} \middle| |z|^2 \right). \quad (2.65)$$

From the differential equation satisfied by the Meijer G-function [53], we have that for large N, n and with $|z|^2 = x$ these functions satisfy the differential equations

$$\left((-1)^m x \prod_{j=1}^m \left(x \frac{d}{dx} + N \right) - \prod_{j=1}^m \left(x \frac{d}{dx} \right) \right) G = 0, \quad \left(x \prod_{j=1}^m \left(x \frac{d}{dx} - n \right) - \prod_{j=1}^m \left(x \frac{d}{dx} \right) \right) G = 0. \quad (2.66)$$

respectively. Being of order m , each admits m linearly independent solutions. Of interest to us are the particular large n, N asymptotic solutions

$$G = \frac{1}{(1 + mx^{1/m})^N}, \quad G = (1 - mx^{1/m})^n. \quad (2.67)$$

We remark that asymptotic properties of the Meijer G-function differential equation is also a feature of the recent studies [29, 32] relating to the singular values of certain products of random matrices. We now use (2.67) in place of the Meijer G-functions in (2.65), and thus in place of w_m in (2.61). A plasma derivation of (2.63) and (2.64) can now be given by going through the argument below (2.2).

The above discussion applies when the matrices in the products have complex entries. Products from the same ensembles but with real quaternion entries allows for a similar analysis. This is because the eigenvalue PDF maintains the same structure as for the $m = 1$ cases, but with a different one-body weight [41], [4],

$$\prod_{l=1}^N w_m^{(4)}(|z_l|)|z_l - \bar{z}_l|^2 \prod_{1 \leq j < k \leq N} |z_k - z_j|^2 |z_k - \bar{z}_j|^2.$$

Moreover, the weight $w_m^{(4)}$ is simply related to $w_m^{(2)}$ appearing in (2.61) [4, Eq. (2.46)], allowing for its replacement by the asymptotic forms in (2.62) and (2.67) as appropriate. In particular, this tells us that the asymptotic densities will be those known for the $m = 1$ case, but with the change of variables $|z| = |w|^{1/m}$.

In the case of products of random matrices from the Ginibre, spherical or truncated unitary matrices with real entries, the structure of the joint eigenvalue PDF (which we recall breaks up into sectors due to the real eigenvalues) again is the same as for the $m = 1$ cases but with different weights [42]. However now the weight for the complex conjugate pairs does not have a closed form beyond the cases $m = 1$ and $m = 2$ [5, 17], so the task of obtaining its asymptotic form remains open.

3 Sum rules

Coulomb systems in general, and the two-dimensional one-component plasma in particular, exhibit a number features characteristic of the long range nature of the pair potential. Many of these features show themselves by way of sum rules for the corresponding correlation functions. By way of example, let $\rho_{(2)}(\vec{r}, \vec{0})$ denote the two-particle correlation function in the bulk of the two-dimensional one-component plasma, and let $\rho_{(2)}^T(\vec{r}, \vec{0}) := \rho_{(2)}(\vec{r}, \vec{0}) - \rho^2$ denote the truncated (or connected) two-particle correlation. For the plasma at inverse temperature β , these satisfy the sequence of sum rules for the moments [46, 54]

$$\frac{1}{\rho} \int_{\mathbb{R}^2} \rho_{(2)}^T(\vec{r}, \vec{0}) d\vec{r} = -1 \quad (3.1)$$

$$\int_{\mathbb{R}^2} r^2 \rho_{(2)}^T(\vec{r}, \vec{0}) d\vec{r} = -\frac{2}{\pi\beta} \quad (3.2)$$

$$\rho \int_{\mathbb{R}^2} r^4 \rho_{(2)}^T(\vec{r}, \vec{0}) d\vec{r} = -\frac{16}{(\pi\beta)^2} \left(1 - \frac{\beta}{4}\right) \quad (3.3)$$

$$\rho^2 \int_{\mathbb{R}^2} r^6 \rho_{(2)}^T(\vec{r}, \vec{0}) d\vec{r} = -\frac{18}{(\pi\beta)^3} (\beta - 6) \left(\beta - \frac{8}{3}\right). \quad (3.4)$$

The first of these has the interpretation that upon a charge being fixed at the origin, the system responds by creating an image charge of equal and opposite total charge; thus rewrite this to read

$$\int_{\mathbb{R}^2} \left(\rho_{(2)}^T(\vec{r}, \vec{0}) + \rho \delta(\vec{r}) \right) d\vec{r} = 0.$$

The second is known as the Stillinger-Lovett sum rule, and can be derived as a consequence of the physical requirement that the plasma perfectly screens an external charge density in the long wavelength limit (see e.g. [25, §15.4.1]). The third is known as the compressibility sum rule, and can be viewed as a refinement of the linear response derivation of (3.2) (see e.g. [25, §14.1.1]). The sixth moment sum rule (3.4), first derived in [46] has recently been shown to result as a consequence of the response to variations in spatial geometry [14, 15].

The bulk truncated two-point correlation function for the complex Ginibre ensemble (which is also shared by all the other ensembles considered in Section 2, in an appropriate scaling and for regions that the density is constant) has the explicit form

$$\rho_{(2)}^T(\vec{r}, \vec{0}) = -\rho^2 e^{-\pi\rho|\vec{r}|^2}, \quad (3.5)$$

with $\rho = 1/\pi$ (see e.g. [25, §15.3.2]). The sum rules (3.1)–(3.4) with $\beta = 2$ are readily verified.

There are also sum rules which contrast the behaviour of the plasma at the boundary to its bulk behaviour. Consider for example the asymptotic form of the charge-charge correlation in the vicinity of the boundary, taken to be $y = 0$ in the scaled limit for definiteness. This quantity is predicted [43] to have a slow decay in the direction of the boundary according to an explicit one on distance squared decay, which in the case of the one-component plasma implies the sum rule for the truncated correlation

$$\rho_{(2)}^T((x_1, y_1), (x_2, y_2)) \Big|_{|x_1 - x_2| \rightarrow \infty} \sim -\frac{f(y_1, y_2)}{2\beta\pi^2(x_1 - x_2)^2}, \quad \text{with} \quad \int_{-\infty}^{\infty} \int_{-\infty}^{\infty} f(y_1, y_2) dy_1 dy_2 = 1. \quad (3.6)$$

For the complex Ginibre ensemble, the scaled edge correlations $\rho_{(k)}^{\text{edge}}$ are defined by

$$\rho_{(k)}^{\text{edge}}((x_1, y_1), \dots, (x_k, y_k)) = \lim_{N \rightarrow \infty} \rho_{(k)}((x_1, -\sqrt{N} + y_1), \dots, (x_k, -\sqrt{N} + y_k)),$$

and explicit computation of this limit gives [26], [25, Prop. 15.3.5]

$$\rho_{(2)}^{\text{edge}}((x_1, y_1), (x_2, y_2)) = \left(H(y_1)H(y_2) - e^{-(x_1 - x_2)^2 - (y_1 - y_2)^2} \left| H\left(\frac{1}{2}(y_1 + y_2 + i(x_1 - x_2))\right) \right|^2 \right), \quad (3.7)$$

where

$$H(z) = \frac{1}{2\pi} \left(1 + \text{erf}(\sqrt{2}z) \right). \quad (3.8)$$

One calculates from this the large $|x_2 - x_1|$ asymptotic form

$$\rho_{(2)}^{T \text{ edge}}((x_1, y_1), (x_2, y_2)) \Big|_{|x_1 - x_2| \rightarrow \infty} \sim -\frac{H'(y_1)H'(y_2)}{4\pi^2(x_1 - x_2)^2}, \quad (3.9)$$

which indeed complies with (3.6) in the case $\beta = 2$, as noted in [26].

The physical origin of the slow decay is the nonzero dipole moment of the screening cloud, due to the presence of the spectral boundary [43]. This can be quantified from the viewpoint of the density profile. With R denoting the boundary of the neutralising background of charge density $-\rho_b$, define the boundary density profile $\rho_{(1)}^{\text{edge}}(r) = \lim_{N, R \rightarrow \infty} \rho_{(1)}(R - r)$. Results in [68, 71] give the dipole moment sum rule

$$\int_{-\infty}^{\infty} r(\rho_{(1)}^{\text{edge}}(r) - \chi_{r>0}\rho_b) dr = -\frac{1}{2\pi\beta}(1 - \beta/4). \quad (3.10)$$

Note that the $\beta = 2$ density profile (3.8) complies with this sum rule.

With the moments of the screening cloud near a boundary in mind, let us consider the limiting truncated two-point correlation in the neighbourhood of the x -axis for the real quaternion Ginibre ensemble. This has been calculated in [47], [25, Ex. 15.9 q.2] to be given by

$$\rho_{(2)}^{T \text{ rQG}}((x_1, y_1), (x_2, y_2)) = -4y_1 y_2 e^{-(x_1^2 + y_1^2) - (x_2^2 + y_2^2)} \left(f(z_1, \bar{z}_2) f(z_2, \bar{z}_1) + f(z_1, z_2) f(\bar{z}_1, \bar{z}_2) \right), \quad (3.11)$$

where $z_1 = x_1 + iy_1$, $z_2 = x_2 + iy_2$ and

$$f(w, z) = \frac{i}{\sqrt{2\pi}} e^{(w^2 + z^2)/2} \text{erf}\left(\frac{z - w}{\sqrt{2}}\right). \quad (3.12)$$

In contrast to the algebraic decay (3.7) of the correlations along the boundary in the complex Ginibre ensemble, the correlation (3.11) decays as a Gaussian in the direction of the x -axis, which for the real

quaternion Ginibre ensemble is the boundary between the eigenvalues in the upper half plane, and their complex conjugate pairs.

Converse to the slow decay (3.7) implying a non-zero dipole moment of the screening cloud, a fast decay implies that all complex (multi-pole) moments of the screening cloud much vanish (see e.g. [54]). As already noted, the complex conjugate eigenvalues behave like image charges, and we know from [23, 43] that in this circumstance we must interpret the screening cloud as the function of $(x_2, y_2) \in \mathbb{R}^2$ specified by

$$\rho_{(2)}^T((x_1, y_1), (x_2, y_2)) + \delta(x_1 - x_2)\delta(y_1 - y_2)\rho_{(1)}((x_2, y_2)). \quad (3.13)$$

Here $\rho_{(2)}^T((x_1, y_1), (x_2, y_2))$ is given by (3.11), which we note is even in y_2 . The quantity $\rho_{(1)}((x_2, y_2))$ is the limiting eigenvalue density for the real quaternion ensemble, which we know from [47], [25, Ex. 15.9 q.2] to be given by

$$\rho_{(1)}^{\text{rqG}}((x, y)) = 2ye^{-(x^2+y^2)}f(z, \bar{z}), \quad (3.14)$$

and is also even in y_2 .

By translation invariance of the system along the x -axis we can set $z = iy_1$. Due to (3.13) being even in y_2 the odd complex moments vanish by symmetry, while the vanishing of the even complex moments requires

$$\int_{\mathbb{R} \times \mathbb{R}_+} w^{2p} \rho_{(2)}^T(z, w) d^2w = -z^{2p} \rho_{(1)}(z), \quad p = 0, 1, \dots \quad (3.15)$$

If we multiply both sides by $\alpha^p/p!$ and sum over $p = 0, 1, \dots$, then substitute (3.13) and (3.14), we obtain the equivalent form

$$\int_{\mathbb{R}^2} ye^{\alpha w^2} e^{-|w|^2} \left(f(iy_1, \bar{w})f(w, -iy_1) + f(iy_1, w)f(-iy_1, \bar{w}) \right) d^2w = e^{-\alpha y_1^2} f(iy_1, -iy_1), \quad (3.16)$$

where $w = x + iy$. To verify this, we substitute (3.12) on the LHS, change variables $x \mapsto x - iy$, write $ye^{-2y^2} = -\frac{1}{4} \frac{d}{dy} e^{-2y^2}$, and integrate by parts with respect to y . The integrand then consists of two terms. Integrating over y in the first of these gives $\pi\delta(x + iy_1)$, and integrating over y in the second gives $\pi i\delta(x - iy_1)$. Thus in both cases the integrations over x are immediate, and the RHS results.

The correlations in the neighbourhood of the real axis for the real Ginibre ensemble [8, 31] can be analysed from an analogous viewpoint. Thus they decay at the rate of a Gaussian, and so Coulomb gas theory predicts that the screening cloud, extended to include image charges, must have the property that all complex moments vanish. Due to the presence of a finite density of real eigenvalues, the screening cloud will involve both the correlation between two eigenvalues in the upper half plane, and an eigenvalue on the real axis (see [30, Eq. (71)]. The verification of this sum rule from the explicit functional form is known from [30, Prop. 4.8].

The plasma analogy valid for the products of random matrices considered in Section 2.5 tells us that it must also be that the complex moments of the screening cloud for the limiting correlation functions in the neighbourhood of the real axis vanishes, although we don't undertake a verification here.

4 Random self-dual non-Hermitian matrices

Dyson's three fold way relates Hermitian matrices $\frac{1}{2}(G + G^\dagger)$ corresponding to square Ginibre matrices G to global time reversal symmetries [16]. There are similarly three classes of chiral ensembles corresponding to the global time reversal symmetry of the Dirac Hamiltonian; see e.g. [70]. This viewpoint was extended by Atland and Zirnbauer [6], who introduced a further four random matrix ensembles motivated by the theoretical description of conductance through a normal metal – superconductor junction in terms of a matrix Bogoliubov – de Gennes Hamiltonian

$$\mathcal{H} = \begin{bmatrix} h & \Delta \\ -\bar{\Delta} & -h^T \end{bmatrix}, \quad \Delta = -\Delta^T.$$

With each block in this matrix of size $N \times N$, N even, the appropriate time reversal symmetry operator T is such that $T^2 = -1$ and has the special structure

$$T = \mathbb{I}_2 \otimes \begin{bmatrix} \mathbb{O}_{N/2} & \mathbb{I}_{N/2} \\ -\mathbb{I}_{N/2} & \mathbb{O}_{N/2} \end{bmatrix} K,$$

where K denotes complex conjugation. The requirement that \mathcal{H} commute with T shows, after rearrangement of rows and columns in the former, that \mathcal{H} has the block form

$$\mathcal{H} = \begin{bmatrix} A & B \\ -\bar{B} & -\bar{A} \end{bmatrix}$$

with $A = A^\dagger$ and $B = -B^T$, and furthermore the elements of A and B real quaternions. As shown in e.g. [25, Ex. 3.3 q.1], the eigenvalue problem for this structure is equivalent to the eigenvalue problem for

$$\begin{bmatrix} \mathbb{O}_N & W \\ W^\dagger & \mathbb{O}_N \end{bmatrix}, \quad (4.1)$$

where W is an $N \times N$ antisymmetric matrix with complex elements, which in turn is equivalent to the eigenvalue problem for

$$\begin{bmatrix} \mathbb{O}_N & D \\ D^\dagger & \mathbb{O}_N \end{bmatrix}, \quad (4.2)$$

where D is an $N \times N$ self-dual matrix — meaning that $D = Z_N D^T Z_N^{-1}$, where $Z_N = \mathbb{I}_{N/2} \otimes \begin{bmatrix} 0 & -1 \\ 1 & 0 \end{bmatrix}$ — with complex elements. On this last point, one can check that if W is antisymmetric, then $Z_N W$ is self dual. A feature of self dual matrices is that their eigenvalues are doubly degenerate.

The structures (4.1) and (4.2) motivated Hastings [40] to investigate the eigenvalue distribution on the non-Hermitian self dual matrix D , constructed according to $D = Z_N W$, where W is a anti-symmetric matrix with all independent entries complex Gaussians with zero mean and fixed standard deviation σ say for both the real and imaginary parts. In contrast to the ensembles of non-Hermitian matrices discussed in Section 2, the eigenvalue PDF for the ensemble of self-dual non-Hermitian complex Gaussian matrices is not known explicitly. Nonetheless, some analysis has been possible under the assumption that the eigenvalues are at large separation, suggesting that in this limit the eigenvalue PDF is well approximated by [40]

$$\prod_{l=1}^N e^{-\frac{1}{2\sigma^2}|z_l|^2} \prod_{1 \leq j < k \leq N} |z_k - z_j|^4, \quad (4.3)$$

up to proportionality. Writing this in the Boltzmann factor form $e^{-\beta U}$ gives that U is given by (1.8), except that the coefficient of the first term is $\frac{1}{8\sigma^2}$, and in distinction to (1.7) the inverse temperature is now $\beta = 4$.

Continuing the investigations already initiated in [40], one would like to show that the properties of the functional form (4.3) are consistent with observed properties of the eigenvalues. The most immediate, already noted in [40], is that in the plasma picture the neutralising background charge density $-\rho_b$ say responsible for the harmonic term in (4.3) must satisfy the Poisson equation $\nabla^2(\frac{1}{8\sigma^2}|z|^2) = 2\pi\rho_b$, and so $\rho_b = \frac{1}{4\pi\sigma^2}$. With N eigenvalues the leading spectral radius is thus predicted to be $2\sigma\sqrt{N}$ and the density to be uniform inside this region — these features are clearly evidenced by a plot of computer generated eigenvalues for matrices from the ensemble (see e.g. [40, Fig. 1. Here $\sigma = 1/\sqrt{2}$]).

The main focus of attention in [40] is the one-point density profile and the two-point correlation function. Regarding the latter, in the plasma system one sees from the explicit functional form (3.6) that for $\beta = 2$ the truncated correlation function is always negative and furthermore is monotonically increasing from its value $-\rho^2$ at $|\vec{r}| = 0$ to its value zero as $|\vec{r}| \rightarrow \infty$. This is consistent with all the moments (3.1)–(3.4) being negative when $\beta = 2$. In contrast, at $\beta = 4$ we see from (3.3) the fourth moment vanishes while (3.4) gives that the 6th moment is positive. Hence, for $\beta = 4$ in the plasma system

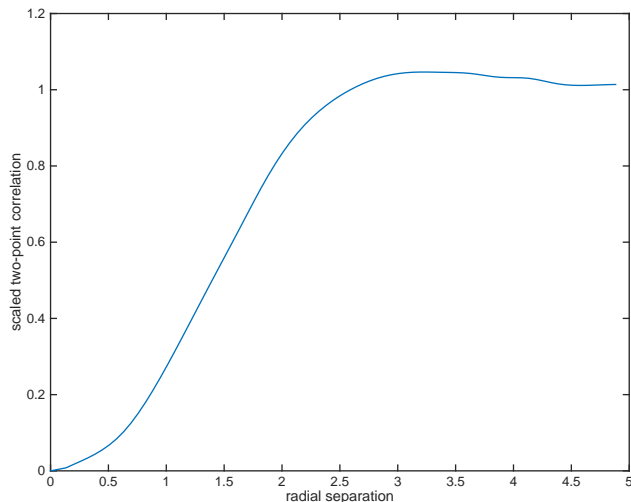


Figure 1: Plot of $\rho_{(2)}^T(\vec{r}, \vec{0})/\rho_b^2$, $\rho_b = 1/2\pi$, as calculated from the simulation of 10^6 non-Hermitian self dual matrix with independent entries standard complex Gaussian entries of size 140×140 , and smoothed using a cubic spline.

the truncated two-point correlation function must become positive and in particular is not monotonic. This behaviour is clearly seen in computer generated plots for finite size systems — see e.g. [69, Fig. 2] — which exhibit a peak in $\rho_{(2)}^T(\vec{r}, \vec{0})$ at $|\vec{r}| \approx 1.7/(\pi\rho_b)^{1/2}$. On the random matrix side, the data presented in [40] was inconclusive due to statistical errors. However, this latter restriction is readily overcome with minimal effort due to the advances in desktop computing (we used Matlab.R2014b). The results, displayed in Figure 1 in the case $\rho_b = 1/(2\pi)$, provide conclusive evidence for a peak in the truncated two-point correlation function at $|\vec{r}| \approx 3$, in agreement with the above quoted peak for the plasma system, although the exact profiles are different. Most evident is that $\rho_{(2)}^T(\vec{r}, \vec{0})$ is proportional to $|\vec{r}|^4$ for small \vec{r} in the plasma system, whereas it appears to vanish in proportion to $|\vec{r}|^2$ for the random matrix ensemble. Note that this latter point does not contradict (4.3), which is only predicted to be accurate for large separations. Although our simulations are accurate at a graphical level, they do not provide reliable estimates of the moments, so the question as to whether the sum rules (3.1)–(3.4) with $\beta = 4$ are valid for the random matrix ensemble remains open.

Next we turn our attention to the radial density. Results from our simulation are displayed in Figure 2. As already noticed in [40], this profile is dramatically different to the scaled edge density $H(r)$ as given by (3.8) for complex Ginibre matrices, or equivalently the plasma system with $\beta = 2$, which does not display any overshoot phenomenon, i.e. a peak in the spectral density near the spectral edge. In the work [12] the overshoot effect observed for the density profile in the non-Hermitian self dual matrix is predicted to be a feature of the two-dimensional one-component plasma system density profile for all $\beta \geq 2$, and the validity of this prediction was given analytic confirmation by a perturbation expansion about $\beta = 2$ in [13]. Note that an overshoot must happen for all $\beta \geq 4$ at least to be consistent with the sum rule (3.10). Comparison of Figure 2 with Figure 1, label ‘2’ in [12], shows quantitative agreement, although there are differences at a qualitative level, for example in Figure 2 the density profile does not dip below the asymptotic value in the direction of the bulk, but does in Figure 1, label ‘2’ in [12].

In summary, our investigation adds to the evidence first presented in [40] that eigenvalues from the ensemble of non-Hermitian self dual matrices have global behaviours consistent with those of the plasma system (4.3), although the precise functional forms of the correlations are different. Due to this latter fact, it is not known if the sum rules (3.10) and (3.1)–(3.2) with $\beta = 4$, characteristic of the plasma system, remain valid for the random matrix ensemble.

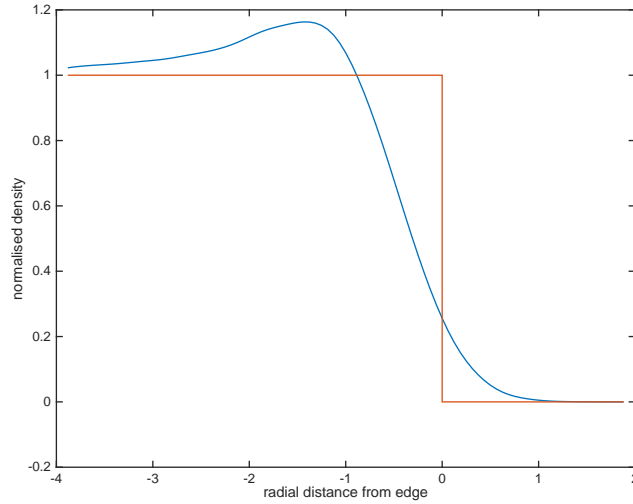


Figure 2: Plot of $\rho_{(1)}(\vec{r})/\rho_b$, $\rho_b = 1/2\pi$, as calculated from the simulation of 10^6 non-Hermitian self dual matrix with independent entries standard complex Gaussian entries of size 140×140 , and smoothed using a cubic spline. The origin has been shifted to $\sqrt{2N}$, which with $\sigma = 1/\sqrt{2}$ is the predicted spectral radius, and as a visual aid a step function density profile inside the spectral radius has been superimposed.

5 Plasma analogy for eigenvalues of a single row and column truncation of CSE matrices

In Section 2.3 truncated unitary matrices were discussed from the viewpoint of plasma analogies for the corresponding eigenvalue PDFs. The unitary matrices considered were from the three classical groups $U(n+N)$, $Sp(2(n+N))$ and $O(n+N)$ with the uniform (Haar) measure. Very recently [49] the explicit eigenvalue PDF for a single row and column truncation of Dyson's three circular ensembles, the COE ($\beta = 1$), CUE ($\beta = 2$) and CSE ($\beta = 4$) has been calculated as

$$\frac{\beta^N}{(2\pi)^N} \prod_{j,k=1}^N (1 - z_j \bar{z}_k)^{\beta/2-1} \prod_{1 \leq j < k \leq N} |z_k - z_j|^2. \quad (5.1)$$

This PDF is supported on $|z_l| < 1$, ($l = 1, \dots, N$).

One recalls (see e.g. [25, Ch. 2]) that the CUE is made up of matrices from $U(N)$ with Haar measure which thus explains why (5.1) with $\beta = 2$ coincides with (2.24) with $n = 1$. On the other hand matrices from the COE and CSE are not the same as matrices from $O(N)$ and $Sp(2N)$. Matrices from the COE are constructed from matrices from $U \in U(N)$ by forming UU^T , while matrices from the CSE are constructed from $U \in U(2N)$ by forming the self dual quaternion matrices $Z_{2N}^{-1}U^T Z_{2N}U$, where Z_{2N} is defined below (4.3). For the truncations considered in [49], N is replaced by $N + 1$, and in the case of the CSE a truncation refers to a row and column of real quaternion elements. As with the original CSE matrices, the resulting matrices again have doubly degenerate eigenvalues.

Of the cases $\beta = 1$ and 4 of (5.1), the case $\beta = 4$, which can be written

$$\left(\frac{2}{\pi}\right)^N \prod_{l=1}^N (1 - |z_l|^2) \chi_{|z_l| < 1} \prod_{1 \leq j < k \leq N} |z_k - z_j|^2 |1 - z_j \bar{z}_k|^2, \quad (5.2)$$

has a plasma interpretation. We consider a one-component plasma formed by placing N unit charges in the unit disk with Neumann boundary conditions. We know (see e.g. [25, §15.9]) that in this setting a

charge at point z' effectively creates an image particle of identical charge at the point $1/\bar{z}'$, and thus the pair potential at point z is

$$-\log(|z - z'| |1 - z\bar{z}'|). \quad (5.3)$$

Consider now a one component plasma system consisting of N particles of unit charge interacting via the pair potential (5.3), and coupled to a background charge density $-\eta$. Due to the particles being restricted to a finite volume (the disk), the background charge density does not have to be neutralising for the particles to remain confined. A short calculation, the result of which is reported in [25, Eq. (15.189)], gives that the total energy of the system, up to an additive constant, is equal to

$$U = \frac{1}{2} \sum_{j=1}^N \left(\pi\eta |z_j|^2 - \log(1 - |z_j|^2) - \sum_{1 \leq j < k \leq N} \log(|z_k - z_j| |1 - z_j \bar{z}_k|) \right).$$

Thus we see that the eigenvalue PDF (5.2) result as the Boltzmann factor $e^{-\beta U}$ of this system with $\beta = 2$, provided we set $\eta = 0$, and thus there is no background charge.

In [25, §15.9] the correlation functions for this same plasma system, except that η was chosen so that the background is neutralising, was computed explicitly. The working therein requires only minor modification to allow for $\eta = 0$. The eigenvalues form a Pfaffian point process [25, Ch. 6]. The one-point function is given by

$$\rho_{(1)}(z) = \frac{1}{\pi} \left(h(|z|^2) - |z|^{4N-2} h(|z|^{-2}) \right), \quad h(s) = \frac{d}{ds} \frac{1 - s^{N+1}}{1 - s}. \quad (5.4)$$

In the limit $N \rightarrow \infty$ with no scaling of the eigenvalues, the Pfaffian reduces to the determinant

$$\rho_{(k)}(z_1, \dots, z_k) = \pi^{-n} \det \left[\frac{1}{(1 - z_j \bar{z}_l)^2} \right]_{j,l=1,\dots,k}. \quad (5.5)$$

This is well known [61] as the correlation function, in the $N \rightarrow \infty$ limit, of the zeros inside the unit disk the random complex polynomials $\sum_{n=0}^N \alpha_n z^n$, where each α_n is an independent standard complex Gaussian, and has the property of being invariant with respect to Möbius transformations which map the unit disk to itself. The correlations (5.5) are the same as those known for (5.1) in the case $\beta = 2$ [50], [25, Ex. 15.7 q.2(iv)], which corresponds to the one-component plasma system in a disk with no background charge.

A further point of interest is to enquire if an explicit functional form analogous to (5.1) for the ensemble obtained by truncating n real quaternion rows and columns of $(N + n) \times (N + n)$ CSE, and so being left with an $N \times N$ real quaternion sub-block, can be obtained for general n, N ? To answer this question, we note that CSE matrices can be characterised as self-dual matrices further constrained to be unitary. Furthermore the fact that the unitary matrices are to be chosen with Haar measure tells us that the underlying matrices are Gaussian — Haar measure results from orthogonalising a basis of Gaussian vectors. For n large and N fixed we thus expect that an $N \times N$ self-dual sub-block can be well approximated to have Gaussian entries. Such an effect is well known for truncations of unitary or orthogonal matrices [45], as can be seen by scaling $G \mapsto \frac{1}{\sqrt{n}} G$ in (2.48) with $n = N$, $M \mapsto n + N$, $\beta = 1$ or 2 and taking $n \rightarrow \infty$. But we know from the discussion of Section 4 that the ensemble of Gaussian self-dual matrices does not allow for explicit determination of its eigenvalue PDF, so we conclude that the sought generalisation of (5.1) is not possible.

Acknowledgements

This research was supported by the Australian Research Council grant DP140102613. I thank Jesper Ipsen for useful feedback relating on an earlier draft. Further, I thank Dong Wang and Jac Verbaarschot at NUS, and the Simons Center for Geometry and Physics (program on Random Matrices, fall semester 2015) respectively, for their hospitality and arranging financial support during my study leave period when ideas for the present paper were being formulated.

References

- [1] K. Adhikari, N.K. Reddy, T.R. Reddy, and K. Saha, *Determinantal point processes in the plane from products of random matrices*, arXiv:1308.6817, 2013.
- [2] G. Akemann and Z. Burda, *Universal microscopic correlations for products of independent Ginibre matrices*, J. Phys. A **45** (2012), 465210.
- [3] G. Akemann, Z. Burda, M. Kieburg, and T. Nagao, *Microscopic correlation functions for products of truncated unitary matrices*, J. Phys. A **47** (2014), 255202.
- [4] G. Akemann and J.R. Ipsen, *Recent exact and asymptotic results for products of independent random matrices*, Acta Physica Polonica B **46** (2015), 1747–1784.
- [5] G. Akemann, M.J. Phillips, and H.-J. Sommers, *The chiral Gaussian two-matrix ensemble of real asymmetric matrices*, J. Phys. A **43** (2010), 085211.
- [6] A. Altland and M.R. Zirnbauer, *Nonstandard symmetry classes in mesoscopic normal-superconducting hybrid compounds*, Phys. Rev. B **55** (1997), 1142–1161.
- [7] G. Ben Arous and O. Zeitoni, *Large deviations from the circular law*, ESIAM: Probability and Statistics **2** (1998), 123?134.
- [8] A. Borodin and C.D. Sinclair, *The Ginibre ensemble of real random matrices and its scaling limit*, Commun. Math. Phys. **291** (2009), 177–224.
- [9] Z. Burda, R.A. Janik, and B. Waclaw, *Spectrum of the product of independent random Gaussian matrices*, Phys. Rev. E **81** (2010), 041132.
- [10] Z. Burda, M.A. Nowak, and A. Swiech, *Spectral relations between products and powers of isotropic random matrices*, Phys. Rev. E **86** (2012), 061137.
- [11] J.M. Caillol, *Exact results for a two-dimensional one-component plasma on a sphere*, J. Phys. Lett. (Paris) **42** (1981), L245–L247.
- [12] T. Can, P.J. Forrester, G. Tellez, and P. Wiegmann, *Singular behavior at the edge of Laughlin states*, Phys. Rev. B **89** (2014), 235137.
- [13] ———, *Exact and asymptotic features of the edge density profile for the one component plasma in two dimensions*, J. Stat. Phys. **158** (2015), 1147–1180.
- [14] T. Can, M. Laskin, and P. Wiegmann, *Fractional quantum Hall effect in a curved space: gravitational anomaly and electromagnetic response*, Phys. Rev. Lett. **113** (2014), 046803.
- [15] ———, *Geometry of quantum Hall states: gravitational anomaly and kinetic coefficients*, arXiv:1411.3105, 2014.
- [16] F.J. Dyson, *The three fold way. Algebraic structure of symmetry groups and ensembles in quantum mechanics*, J. Math. Phys. **3** (1962), 1199–1215.
- [17] A. Edelman, *The probability that a random real Gaussian matrix has k real eigenvalues, related distributions, and the circular law*, J. Multivariate. Anal. **60** (1997), 203–232.
- [18] A. Edelman and E. Kostlan, *How many zeros of a random polynomial are real?*, Bull. Amer. Math. Soc. **32** (1995), 1–37.
- [19] J. Feinberg and A. Zee, *Non-Gaussian non-Nermitian random matrix theory: Phase transition and addition formalism*, Nucl. Phys. B, **501** (1997), 643?669.
- [20] J. Fischmann, W. Bruzda, B.A. Khoruzhenko, H.-J. Sommers, and K. Zyczkowski, *Induced Ginibre ensemble of random matrices and quantum operations*, J. Phys. A **45** (2012), 075203.
- [21] J. Fischmann and P.J. Forrester, *One-component plasma on a spherical annulus and a random matrix ensemble*, J. Stat. Mech. **2011** (2011), P10003.
- [22] J.A. Fischmann, *Eigenvalue distributions on a single ring*, Ph.D. thesis, Queen Mary, University of London, 2012.
- [23] P.J. Forrester, *The two-dimensional one-component plasma at $\Gamma = 2$: metallic boundary*, J. Phys. A **18** (1985), 1419–1434.
- [24] ———, *Quantum conductance problems and the Jacobi ensemble*, J. Phys. A. **39** (2006), 6861–6870.
- [25] ———, *Log-gases and random matrices*, Princeton University Press, Princeton, NJ, 2010.
- [26] P.J. Forrester and G. Honner, *Exact statistical properties of the zeros of complex random polynomials*, J. Phys. A **32** (1999), 2961–2981.

- [27] P.J. Forrester and B. Jancovici, *Two-dimensional one-component plasma in a quadrupolar field*, Int. J. Mod. Phys. A **11** (1996), 941–949.
- [28] P.J. Forrester and M. Krishnapur, *Derivation of an eigenvalue probability density function relating to the Poincaré disk*, J. Phys. A **42** (2009), 385204 (10pp).
- [29] P.J. Forrester and D.-Z. Liu, *Raney distributions and random matrix theory*, J. Stat. Phys. **158** (2015), 1051–1082.
- [30] P.J. Forrester and A. Mays, *Pfaffian point processes for the Gaussian real generalised eigenvalue problem*, Prob. Theory and Rel. Fields **154** (2012), 1–47.
- [31] P.J. Forrester and T. Nagao, *Eigenvalue statistics of the real Ginibre ensemble*, Phys. Rev. Lett. **99** (2007), 050603.
- [32] P.J. Forrester and D. Wang, *Muttalib–borodin ensembles in random matrix theory — realisations and correlation functions*, arXiv:1502.07147.
- [33] P. Di Francesco, M. Gaudin, C. Itzykson, and F. Lesage, *Laughlin’s wave functions, Coulomb gases and expansions of the discriminant*, Int. J. Mod. Phys. A **9** (1994), 4257–4351.
- [34] Y.V. Fyodorov, B.A. Khoruzhenko, and H.-J. Sommers, *Almost-Hermitian random matrices: crossover from Wigner-Dyson to Ginibre eigenvalue statistics*, Phys. Rev. Lett. **79** (1997), 557–560.
- [35] Y.V. Fyodorov and H.-J. Sommers, *Random matrices close to hermitian or unitary: overview of methods and results*, J. Phys. A **36** (2003), 3303–3347.
- [36] J. Ginibre, *Statistical ensembles of complex, quaternion, and real matrices*, J. Math. Phys. **6** (1965), 440–449.
- [37] F. Götze, K. Kösters, and A. Tikhomirov, *Asymptotic spectra of matrix-valued functions of independent random matrices and free probability*, arXiv:1408.1732.
- [38] F. Götze and A. Tikhomirov, *On the asymptotic spectrum of products of independent random matrices*, arXiv:1012.2710, 2010.
- [39] J. H. Hannay, *Chaotic analytic zero points: exact statistics for those of a random spin state*, J. Phys. A **29** (1996), L101–L105.
- [40] M.B. Hastings, *Eigenvalue distribution in the self-dual non-Hermitian ensemble*, J. Stat. Phys. **103** (2001), 903–913.
- [41] J.R. Ipsen, *Products of independent quaternion Ginibre matrices and their correlation functions*, J. Phys. A **46** (2013), 265201.
- [42] J.R. Ipsen and M. Kieburg, *Weak commutation relations and eigenvalue statistics for products of rectangular random matrices*, Phys. Rev. E **89** (2014), 032106.
- [43] B. Jancovici, *Classical Coulomb systems near a plane wall. II*, J. Stat. Phys. **29** (1982), 263–280.
- [44] B. Jancovici and G. Téllez, *Two-dimensional Coulomb systems on a surface of constant negative curvature*, J. Stat. Phys. **91** (1998), 953–977.
- [45] T. Jiang, *How many entries of a typical orthogonal matrix can be approximated by independent normals?*, Ann. Probab. **34** (2006), 1497–1529.
- [46] P. Kalinay, P. Markos, L. Samaj, and I. Travenec, *The sixth-moment sum rule for the pair correlations of the two-dimensional one-component plasma: exact results*, J. Stat. Phys. **98** (2000), 639–666.
- [47] E. Kanzieper, *Eigenvalue correlations in non-Hermitian symplectic random matrices*, J. Phys. A **35** (2002), 6631–6644.
- [48] B.A. Khoruzhenko, H.-J. Sommers, and K. Zyczkowski, *Truncations of random orthogonal matrices*, Phys. Rev. E **82** (2010), 040106(R) (4pp).
- [49] R. Killip and R. Kozhan, *Matrix models and eigenvalue statistics for truncations of classical ensembles of random unitary matrices*, arXiv:1501.05160, 2015.
- [50] M. Krishnapur, *Zeros of random analytic functions*, Ann. Prob. **37** (2009), 314–346.
- [51] P. Leboeuf, *Random matrices, random polynomials and coulomb systems*, J. de Physique IV France **10** (2000), Pr5–45.
- [52] N. Lehmann and H.-J. Sommers, *Eigenvalue statistics of random real matrices*, Phys. Rev. Lett. **67** (1991), 941–944.
- [53] Y.L. Luke, *The special functions and their approximations, Vol. I*, Academic Press, New York-London, 1969.

- [54] Ph. A. Martin, *Sum rules in charged fluids*, Rev. Mod. Phys. **60** (1988), 1075–1127.
- [55] A. Mays, *A geometrical triumvirate of real random matrices*, Ph.D. thesis, University of Melbourne, 2012.
- [56] ———, *A real quaternion spherical ensemble of random matrices*, J. Stat. Phys. **153** (2013), 48–69.
- [57] M.L. Mehta, *Random matrices*, 2nd ed., Academic Press, New York, 1991.
- [58] H.H. Nguyen and S. O’Rourke, *The elliptic law*, Int. Math. Res. Notices **2014** (2014), rnu174.
- [59] S. O’Rourke and A. Soshnikov, *Products of independent non-Hermitian matrices*, Electron. J. Prob. **16** (2011), 2219–2245.
- [60] L. Pastur and M. Shcherbina, *Eigenvalue distribution of large random matrices*, American Mathematical Society, Providence, RI, 2011.
- [61] Y. Peres and B. Virág, *Zeros of the i.i.d. Gaussian power series: a conformally invariant determinantal process*, Acta. Math. **194** (2005), 1–35.
- [62] D. Petz and F. Hiai, *Logarithmic energy as entropy functional*, Contemp. Math. **217** (1998), 205–221.
- [63] C.E. Porter, *Statistical theories of spectra: fluctuations*, Academic Press, New York, 1965.
- [64] E.B. Saff and V. Totik, *Logarithmic potentials with external fields*, Springer, Berlin, 1997.
- [65] E. Sandier and S. Serfaty, *2D Coulomb gases and the renormalized energy*, Ann. Prob. **43** (2015), 2026–2083.
- [66] H.-J. Sommers, A. Crisanti, H. Sompolinsky and Y. Stein, *Spectrum of large random asymmetric matrices*, Phys. Rev. Lett. **60** (1988) 1895–1898
- [67] T. Tao and V. Vu, *From the Littlewood-Offord problem to the circular law: universality of the spectral distribution of random matrices*, Bull. Amer. Math. Soc. **46** (2009), 377–396.
- [68] G. Telléz and P.J. Forrester, *Expanded Vandermonde powers and sum rules for the two-dimensional one-component plasma*, arXiv:1204.6003.
- [69] ———, *Finite size study of the 2dOCP at $\Gamma = 4$ and $\Gamma = 6$* , J. Stat. Phys. **97** (1999), 489–521.
- [70] J.J.M. Verbaarschot, *The spectrum of the Dirac operator near zero virtuality for $N_c = 2$ and chiral random matrix theory*, Nucl. Phys. B **426** (1994), 559–574.
- [71] P. Wiegmann, *Nonlinear hydrodynamics and fractionally quantized solitons at the fractional quantum Hall edge*, Phys. Rev. Lett. **108** (2012), 206810.
- [72] E.P. Wigner, *Statistical properties of real symmetric matrices with many dimensions*, Can. Math. Congr. Proc., Univ. Toronto Press (1957), 174.
- [73] A. Zabrodin and P. Wiegmann, *Large- N expansion in the 2D Dyson gas*, J. Phys. A **39** (2006), 8933–8963.
- [74] K. Zyczkowski and H.-J. Sommers, *Truncations of random unitary matrices*, J. Phys. A **33** (2000), 2045–2057.